

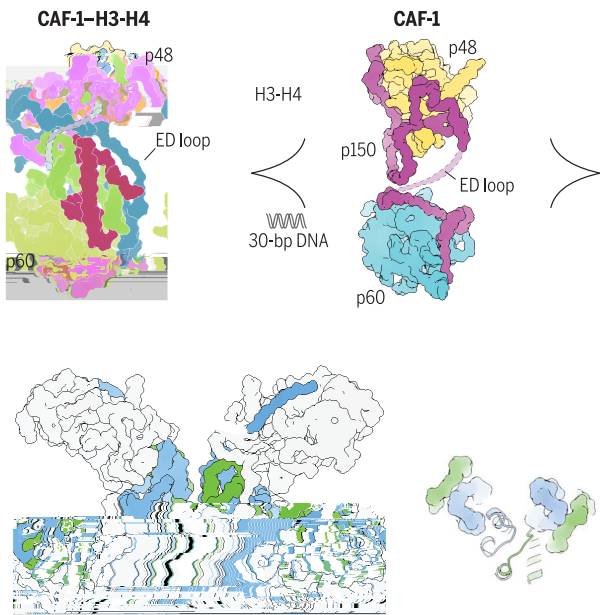
RESEARCH ARTICLE SUMMARY

STRUCTURAL BIOLOGY

Structural insights into histone binding and nucleosome assembly by chromatin assembly factor 1

Chao-Pei Liu<sup>\*†</sup>, Zhenyu Yu<sup>†</sup>, Jun Xiong<sup>†</sup>, Jie Hu<sup>†</sup>, Aoqun Song<sup>†</sup>, Dongbo Ding<sup>†</sup>, Mingzhu Wang, Juan Yu, Peini Hou, Kangning Zeng, Zhenyu Li, Zhuqiang Zhang, Wei Li, Zhiguo Zhang, Bing Zhu<sup>\*</sup>, Guohong Li<sup>\*</sup>, Rui-Ming Xu<sup>\*</sup>

<p><b>INTRODUCTION:</b></p> <p>CAF-1 (CAF-1) is a histone chaperone that facilitates nucleosome assembly by binding to H3-H4 dimers and DNA. The structure of CAF-1 in complex with H3-H4 and DNA provides insights into its mechanism of action.</p>	<p><b>RATIONALE:</b></p> <p>CAF-1 is a histone chaperone that facilitates nucleosome assembly by binding to H3-H4 dimers and DNA. The structure of CAF-1 in complex with H3-H4 and DNA provides insights into its mechanism of action.</p>
<p><b>RESULTS:</b></p> <p>The structure of CAF-1 in complex with H3-H4 and DNA reveals the binding sites and interactions between the protein and the histone core. The ED loop is a key structural element that interacts with the H3-H4 dimer and DNA.</p>	<p><b>RESULTS:</b></p> <p>The structure of CAF-1 in complex with H3-H4 and DNA reveals the binding sites and interactions between the protein and the histone core. The ED loop is a key structural element that interacts with the H3-H4 dimer and DNA.</p>



The list of author affiliations is available in the full article online.  
 \*Corresponding author. Email: liuchaopei@ibp.ac.cn (C.-P.L.); zhubing@ibp.ac.cn (B.Z.); liguohong@ibp.ac.cn (G.L.); rmxu@ibp.ac.cn (R.-M.X.)  
 †These authors contributed equally to this work.  
 Cite this article as C.-P. Liu *et al.*, *Science* **381**, eadd8673 (2023). DOI: 10.1126/science.add8673

**S** READ THE FULL ARTICLE AT  
<https://doi.org/10.1126/science.add8673>

# Structural insights into histone binding and nucleosome assembly by chromatin assembly factor-1

Chao-Pei Liu<sup>1\*</sup>, Zhenyu Yu<sup>1†</sup>, Jun Xiong<sup>1†</sup>, Jie Hu<sup>1†</sup>, Aoqun Song<sup>1†</sup>, Dongbo Ding<sup>1†</sup>, Cong Yu<sup>1,2</sup>, Na Yang<sup>3</sup>, Mingzhu Wang<sup>4</sup>, Juan Yu<sup>1</sup>, Peini Hou<sup>1</sup>, Kangning Zeng<sup>1,5</sup>, Zhenyu Li<sup>6</sup>, Zhuqiang Zhang<sup>1</sup>, Xinzheng Zhang<sup>1,5</sup>, Wei Li<sup>1,5</sup>, Zhiguo Zhang<sup>7</sup>, Bing Zhu<sup>1,5,8\*</sup>, Guohong Li<sup>1,5\*</sup>, Rui-Ming Xu<sup>1,2,5\*</sup>

Chromatin inheritance entails de novo nucleosome assembly after DNA replication by chromatin assembly factor-1 (CAF-1). Yet direct knowledge about CAF-1's histone binding mode and nucleosome assembly process is lacking. In this work, we report the crystal structure of human CAF-1 in the absence of histones and the cryo-electron microscopy structure of CAF-1 in complex with histones H3 and H4. One histone H3-H4 heterodimer is bound by one CAF-1 complex mainly through the p60 subunit and the acidic domain of the p150 subunit. We also observed a dimeric CAF-1-H3-H4 supercomplex in which two H3-H4 heterodimers are poised for tetramer assembly and discovered that CAF-1 facilitates right-handed DNA wrapping of H3-H4 tetramers. These findings signify the involvement of DNA in H3-H4 tetramer formation and suggest a right-handed nucleosome precursor in chromatin replication.

**T**he chromatin assembly factor-1 (CAF-1) is a heterotrimeric complex composed of three subunits: p150, p60, and p48. It is essential for the de novo assembly of nucleosomes after DNA replication. In this study, we determined the crystal structure of human CAF-1 in the absence of histones and the cryo-electron microscopy structure of CAF-1 in complex with histones H3 and H4. The crystal structure shows that CAF-1 is a heterotrimeric complex with a central p60 subunit and two p150 subunits. The p60 subunit is bound to the p150 subunits through its acidic domain. The cryo-EM structure shows that CAF-1 is bound to the H3-H4 heterodimer through its p60 subunit and the acidic domain of the p150 subunit. We also observed a dimeric CAF-1-H3-H4 supercomplex in which two H3-H4 heterodimers are poised for tetramer assembly and discovered that CAF-1 facilitates right-handed DNA wrapping of H3-H4 tetramers. These findings signify the involvement of DNA in H3-H4 tetramer formation and suggest a right-handed nucleosome precursor in chromatin replication.

CAF-1 is a heterotrimeric complex composed of three subunits: p150, p60, and p48. It is essential for the de novo assembly of nucleosomes after DNA replication. In this study, we determined the crystal structure of human CAF-1 in the absence of histones and the cryo-electron microscopy structure of CAF-1 in complex with histones H3 and H4. The crystal structure shows that CAF-1 is a heterotrimeric complex with a central p60 subunit and two p150 subunits. The p60 subunit is bound to the p150 subunits through its acidic domain. The cryo-EM structure shows that CAF-1 is bound to the H3-H4 heterodimer through its p60 subunit and the acidic domain of the p150 subunit. We also observed a dimeric CAF-1-H3-H4 supercomplex in which two H3-H4 heterodimers are poised for tetramer assembly and discovered that CAF-1 facilitates right-handed DNA wrapping of H3-H4 tetramers. These findings signify the involvement of DNA in H3-H4 tetramer formation and suggest a right-handed nucleosome precursor in chromatin replication.

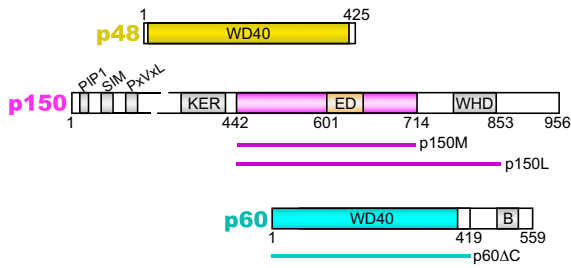
(9). B 60 48  
D40-  
β- (F . 1A). 60  
D A  
(26-28). C- A Fl-  
(B )  
H3-H4 CAF-1 (29).  
, 60 H3-H4  
CAF-1' (9, 30).  
48 H3-H4  
(23, 31).  
CAF-1'  
(32, 33).  
CAF-1  
(30, 34-36). CAF-1  
(-E ) CAF-1 H3-H4.  
CAF-1 H3-H4

## Results

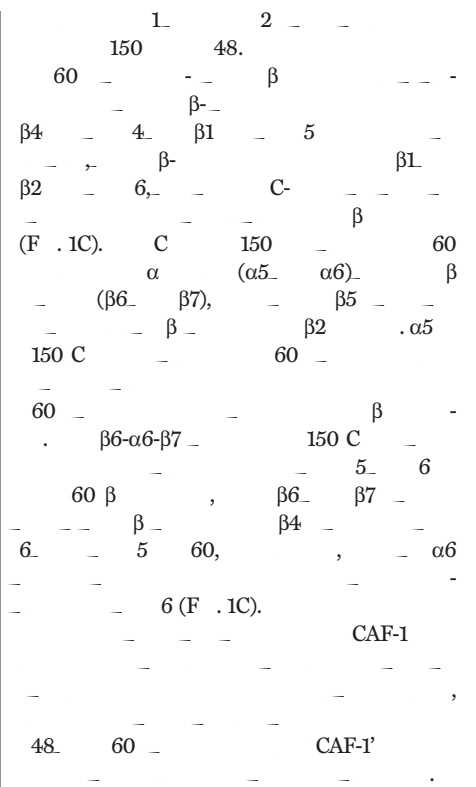
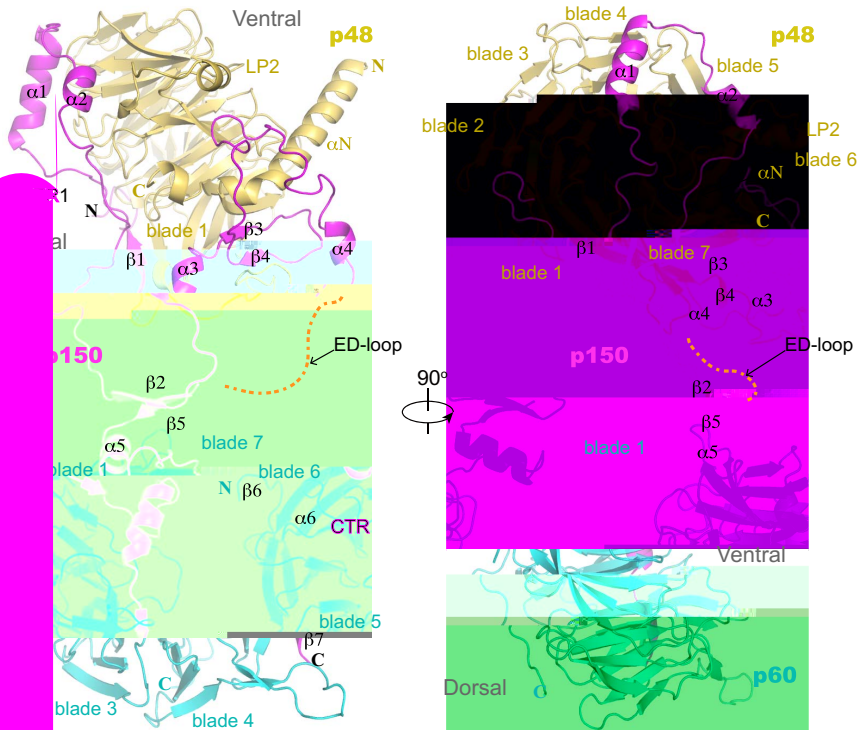
### Overall structure of the CAF-1 complex

CAF-1  
150  
150 ,  
ED  
C- ( C ,  
) 150 ,  
C- (F . 1A).  
(F . 1B),  
150 , 60  
C- 140-  
48, CAF1- C  
(C222<sub>1</sub>, C2<sub>2</sub>, 2<sub>1</sub>), 3.4- 3.6-

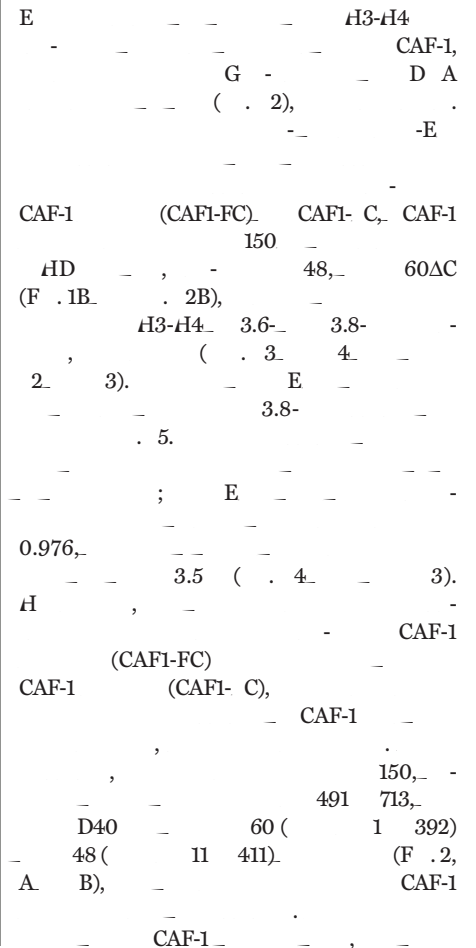
**A**



**C**



**Structure of CAF-1 bound to histone H3-H4**

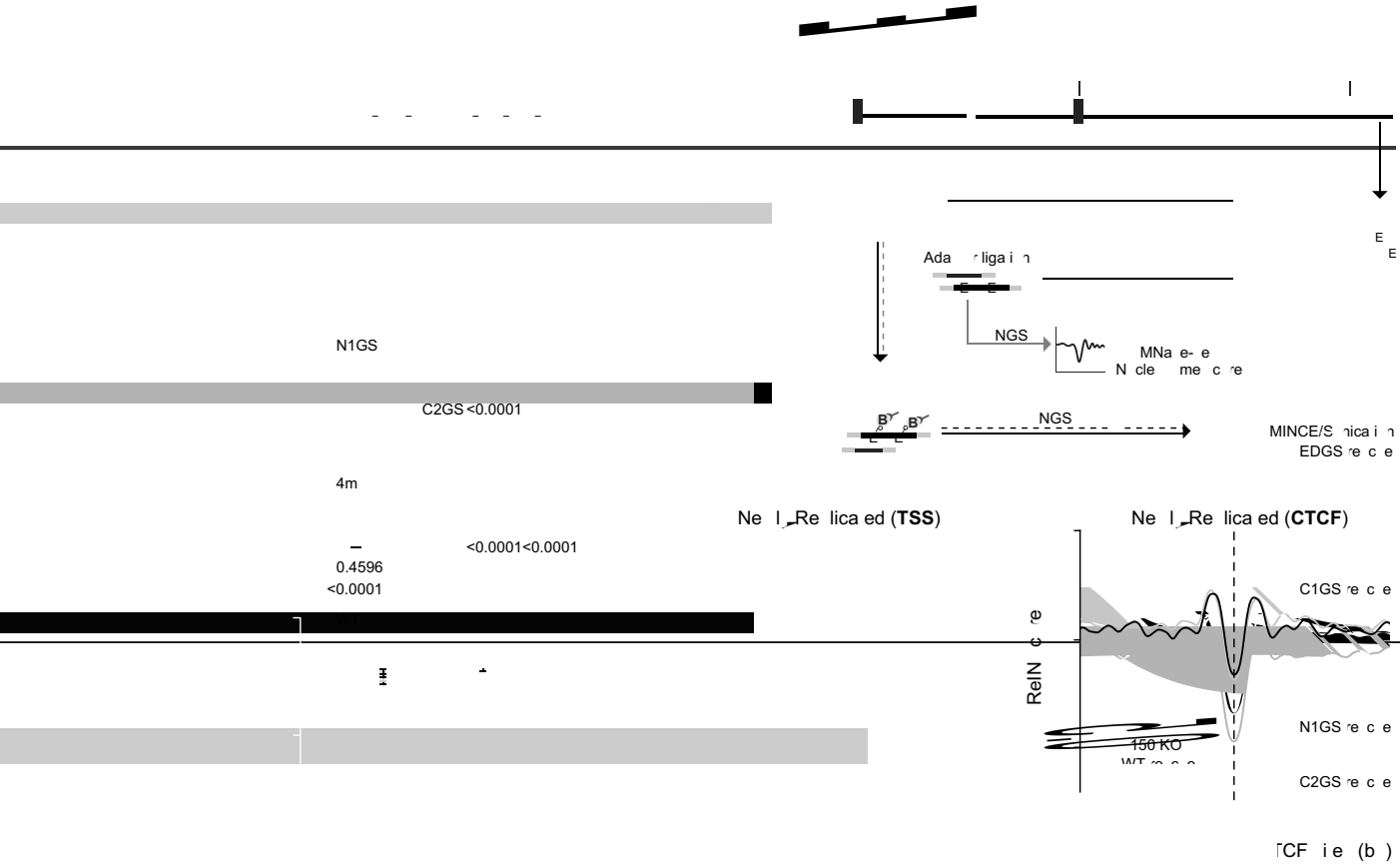


CAF-1  
H3-H4, / 30-  
D A (D A<sub>30</sub>),  
E A CAF-1  
H3-H4  
(F . 2, A B). C  
, 48 60  
(F . 2C.  
1). 60  
, 48  
60  
H3-H4.  
F , 150 α4  
70 (F . 2C.  
1).  
H3-H4 , 1  
150 , 48  
α1  
1 2 , 2  
48

(F . 2B). 50-  
C 150,  
ED ,  
H3-H4 (F . 2A

ED- H3-H4 ,  
H3-H4 ,  
H4 α1 H3 D A  
(F .3A). ED 150. H3-H4  
C 2. H3-  
H4 ( . 6A) (37-39), H3-H4  
D A D A  
CAF-1 C 2 H3-H4  
H3-H4 , (40).  
32- ,  
ED  
-E ,  
ED  
H3-H4 ( . 5B).  
ED  
C- ED  
ED- 1 ( 601 617) ED-C1 ( 618 632), C-  
, ED-C2 ( 617 646)  
α5A, G  
(F .3A). H α5A  
α1-α2 H3 α2-α3 H4 (F .  
2D). G (F .3B)  
(F .3C . 6B)  
ED-C1G ED-C2G  
CAF-1  
ED-  
(EDG ), ED- 1G  
.A  
ED-C1 4 , E628  
(G<sup>628</sup>→ ), D629 , E630 , D632G  
G  
(F . 3, B C).  
F , ED- 1  
H4 ED-C1 ED-C2  
H3 (F .3A),  
H3 H4 . A  
ED A<sup>63</sup>,  
A<sup>69</sup>, A<sup>83</sup> H3 (H3-3A)  
A<sup>35</sup>, A<sup>39</sup>,<sup>44</sup> H4 (H4-3A)  
H3-3A 8

GST  
C1GS  
N1GS  
EDGS  
C2GS



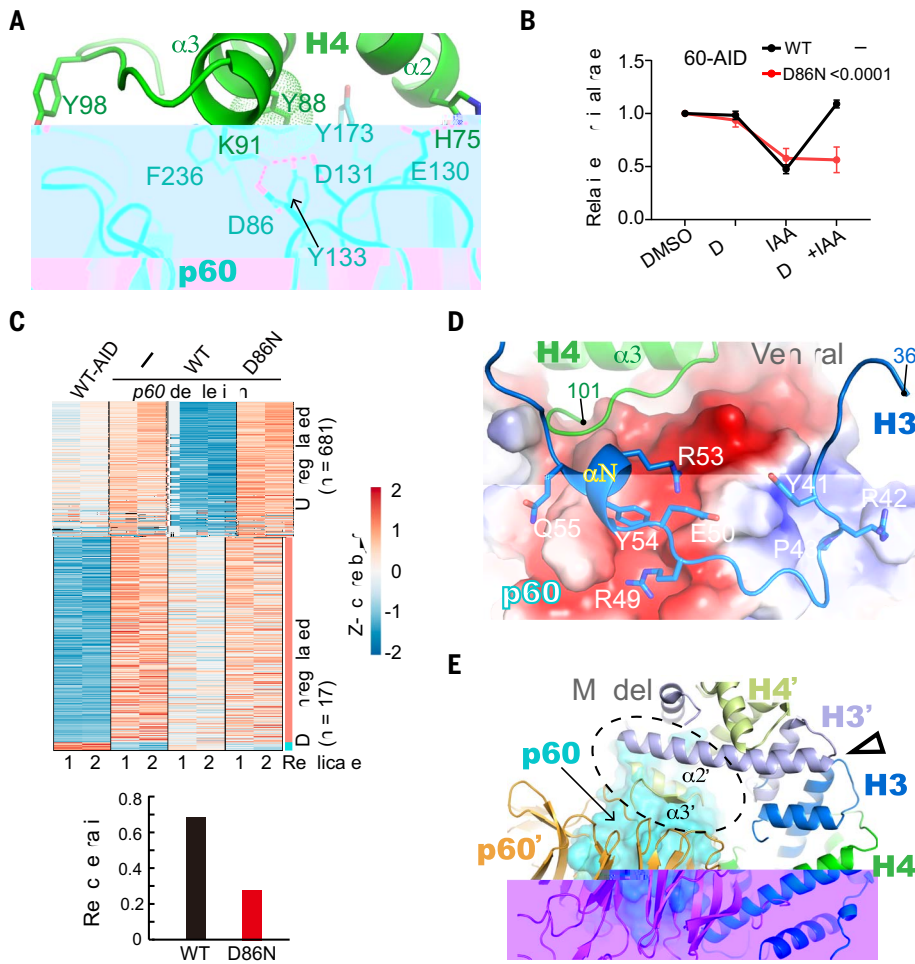
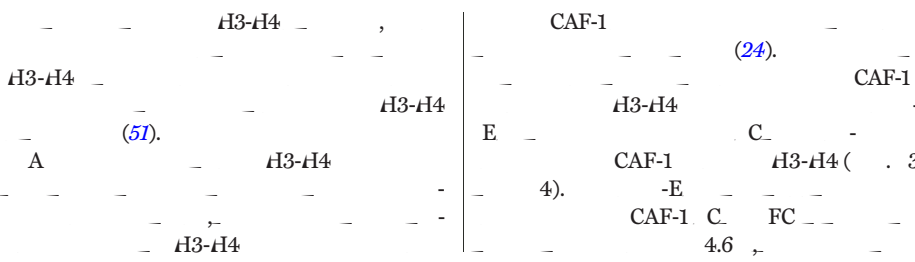


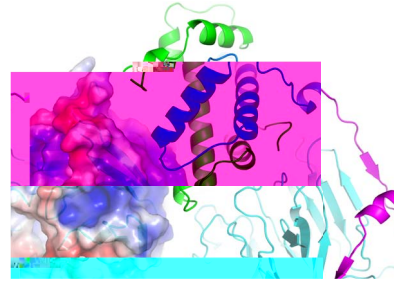
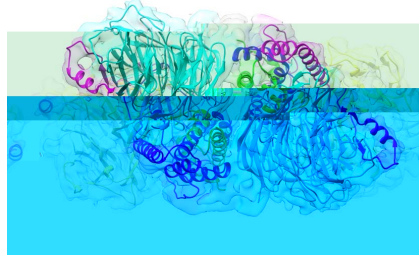
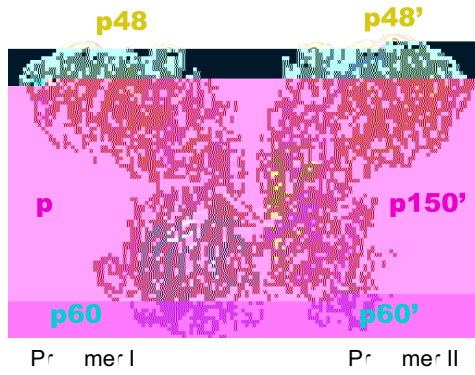
**Fig. 4. Interactions between p60 and histone H3-H4.** (A) Histone H4–p60 interaction at the center of the ventral surface of p60. Involved residues are shown in a stick model. Magenta dashed lines indicate potential hydrogen bonds. Tyr<sup>88</sup> of H4, which is situated in the central basin of the ventral face of p60, is superimposed with a dots model. F, Phe; P, Pro; Q, Gln; Y, Tyr. (B) Cell proliferation activity of WT p60 and the D86N mutation assayed in the same was as in Fig. 3D. Error bars represent SEM from three biological replicates. (C) Heatmaps showing differentially expressed genes (DEGs) in p60-depleted and rescued cells versus WT-AID HAP1 cells. Two biological replicates were performed for each experiment. The bottom panel shows the rescue ratios of transcriptional changes, which is defined as  $1 - \frac{\#(A \cap B)}{\#(A)}$ , where  $A$  is the set of DEGs from p60 depletion and  $B$  is the set of DEGs from rescue expression of WT or D86N p60 constructs. The  $\#$  function gives the number of genes in the set. (D) Interaction between histone H3 (dark blue) and p60. Histones H3-H4 are drawn in a cartoon model, with involved H3 residues depicted in a stick model. p60 is shown in a surface model colored according to electrostatic potential (negative, red; neutral, white; positive, blue) with the display range of  $-3$  to  $+3 k_B T/e$ , where  $k_B$  is the Boltzmann constant and  $T$  and  $e$  are the temperature and electron charge in SI units, respectively. (E) Docking of a second CAF-1–H3–H4 complex (p60', orange; H3', light blue; H4', light green) to model the formation of a H3–H4 tetramer between the H3'–H4' heterodimer and the H3–H4 heterodimer from the first CAF-1–H3–H4 complex, which is colored as in Fig. 2B, results in steric clashes between H4' and p60 (indicated with a dashed oval), and p60' with p60 and H4. The black triangle indicates the H3–H3' dimerization interface. p150 and p48 have been removed for viewing clarity.



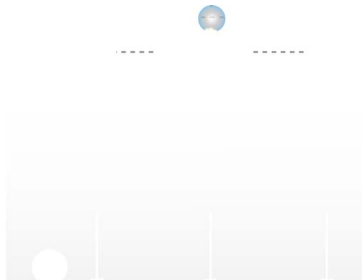
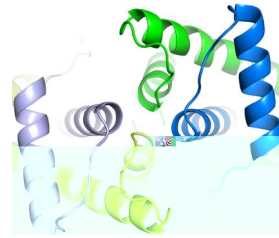
CAF-1–H3–H4  
(F . 5A . . 3- 4). A EC- A  
( . . . . . )  
-E . . . . .  
CAF-1–H3–H4  
, C, C,  
FC . . . . .  
8). A . . . . .  
CAF-1–H3–H4  
D A . . . . .  
CAF-1–H3–H4  
, . . . . .  
60 . . . . .  
60 . . . . .  
C- . . . . .  
β3–β4 . . . . .  
C- . . . . .  
(F . 5C).  
H3 . . . . .  
H4 . . . . .  
(F . 5D). H3–H4  
“ . . . . .  
60 . . . . .  
60 . . . . .  
D A, . . . . .  
H3–H4 . . . . .  
CAF-1 . . . . .  
(8, 35, 52).  
**CAF-1 facilitates the assembly of a right-handed ditetrasome**  
D . . . . .  
H3–H4 D A CAF-1  
D A . . . . .  
H3–H4 . . . . .  
CAF-1 C,  
CAF-1 C,  
601 D A  
H3–H4, . . . . .  
2 . . . . .  
147- . . . . .  
50 . . . . .  
C, . . . . .  
-E . . . . .  
1 . . . . .  
G F ( . . . . .  
9A). F . . . . .  
CAF-1-  
CAF-1-  
3.5- . . . . .  
3.8- . . . . .  
( . 9, B F; . . . . .  
2 . . . . .  
CAF-1 . . . . .  
CAF-1 . . . . .  
5.6 . . . . .  
( . 10 . . . . .  
2). . . . .  
H3–H4 . . . . .  
(53); . . . . .  
CAF-1 . . . . .  
( . 11 . . . . .  
3). C -E . . . . .  
CAF-1 . . . . .  
3.8- 6.6- . . . . .  
. B . . . . .

Downloaded from https://www.science.org at Institute of Biophysics, CAS on September 15, 2025

A



-CAF-1-	-CAF-1-	(F . 6B). A	2. 3(F . 6C). A
FC	CAF-1	H3 $\alpha$ 2. H4 $\alpha$ 3	D A H4
II, E.	F).	(F . 6B).	3. 4. D A
	CAF1- C	H3-H4	60
	CAF-1-	CAF-1-	(E A) ( . 13A). F
	108- D A	45	, $\alpha$
	H3-H4	D A	H3 H3-H4
	(F . 6A)		D A, H4
12). E	H3-H4	(F . 6A).	$\alpha$ 1 H4 $\alpha$ 2
		60	H3-
H4	$\alpha$ 2- $\alpha$ 3	C- H4 $\alpha$ 2	H4 ( . 13B).
		$\beta$	



H3-H4  
H<sub>1</sub>,  
D A.  
60  
β6-α6-β7 150 C,  
60  
CAF-1  
CAF-1 H3-H4;  
150 48 (F  
6A).  
CAF-1  
H3-H4 D A. A 5.6-  
-E 2  
(. 10 2),  
60- 150  
(. 10E). F 2  
48 60 D40  
(. 10C).  
A CAF-1,  
D A, H3-H4  
(8).  
CAF-1- D A  
(F )  
D A  
50 C.  
*et al. (54),*

**Materials and methods**  
**Plasmid construction**

CAF-1  
 E B 1 ( )  
 G  
 150 C- 6 H  
 60 48  
 .A  
 G  
 150 . F  
 CAF-1  
 , D A 150  
 A , D A  
 60 48  
 .A  
 A  
 150  
 H3.1 H4  
 CDFD 1 ( )  
 150  
 60 H3.1 H4  
 D-  
 ( B , -101)  
 .A  
 D A  
 A D A D2  
 (44),  
 1 D A 232(C I-  
 , .72834). AA I-(F74G)  
 D A I-  
 CAG-F -E 2(A , .68460)  
 C (B ) F -E 2  
 AAVSI  
 C 2(A , .  
 52961)  
 .A A D- 2A-  
 p150 p60  
 C -C 9-  
 p150-A D  
 (59),  
 p60-A D  
 p150 p60 C 2.  
 F 150 60 ,  
 p150 p60 D A C -  
 C 9(A , .50661) C  
 C 9  
 CA -  
 64 B. (A , .61425). 150 60  
 ( C ).

**Protein expression and purification**  
 CAF-1 21  
 B -B

( ) CAF-1  
 CAF-1 293F  
 (HE 293F) .A 500 HE 293F  
 0.5  
 CAF-1 (1:1:1 )  
 2 48  
 37 C.  
 CAF-1  
 (CAF1- C) G 150  
 ( 442 714), 60ΔC-H , 48-H ,  
 20 -HC, H 7.5,  
 500 C, 5 ,1  
 ( F)  
 C ,  
 A 30 4 C,  
 500 ,1 ED A  
 (D )  
 A , (G H) (GE H -  
 ) A-500 (20  
 -HC, H 7.5, 500 C, 1 ED A,  
 1 D ) 2 G H  
 A-500,  
 30 G H. G  
 100 C (GE H - )  
 0.1 2 C .E  
 D  
 ( D - AGE),  
 CAF1- C  
 H 16/60  
 200 (GE H - )  
 A-500. E  
 CAF1- C  
 20 /  
 -80 C  
 CAF-1 (CAF1- C)  
 150 ( 442-853) ,  
 HD ,  
 .F CAF-1 (CAF1-FC)  
 G ( G) 2 ,  
 A-500.

A-500.  
 6 10/300 G (GE

H ) -  
 A-2000, 2 C. C-  
 6 H 48 60ΔC  
 , A,  
 H 16/60 H 200  
 H3.1-H4  
 CDFD 1-  
 H3.1-H4 Escherichia coli B 21  
 C (DE3)  
 0.5 -β-D-  
 ( G) 37 C 4  
 H  
 5- (GE H - ),  
 2 C.  
**Crystallization**  
 CAF1- C  
 20 C 1.0 μ  
 (7 10 / )  
 1.0 μ 8% ( / )  
 , H 6.0, 20% ( / ) EG 3350.  
 7% , H 6.0,  
 22% ( / ) EG 3350, 0.12  
 0.05 4 C.  
 (3 5 / ) 15 25% ( / )  
 EG3350 0 0.2  
 7% , H 6.0, 18% ( / ) EG  
 3350, 0.12 0.13  
 3 5 .C  
 15%  
**X-ray diffraction data collection, structure determination, and refinement**  
 D E ( F )  
 B 17 315 CCD  
 (AD C) 0.97915  
 B 19 6  
 0.97853 .D  
 H 2000  
 (60). C222<sub>1</sub>  
 2<sub>1</sub> C2 C222<sub>1</sub>, 2<sub>1</sub>-  
 C2 3.5-, 3.6-, 3.4-  
 C222<sub>1</sub>  
 ( )  
 HA E (61)  
 48/ BB 4 D B (DB)  
 D 3GFC D40-  
 C. 1( DB D3F 0).

Downloaded from https://www.science.org at Institute of Biophysics, CAS on September 15, 2025

150 48 60. A  
 CAF1- C (62),  
 HE (63).  
 R 0.225 0.257,  
 96.8 3.2%  
 463 713  
 150, 1 394 60,  
 7 411 48.  
 150 607 657,  
 100 111 60.  
 C222<sub>1</sub>  
 . F ,  
 (64). D  
 I.  
**DNA preparation**  
 A30- D A (D A<sub>30</sub>)  
 (H C)-  
 D A  
 ( : 5'-G AA CCCC GGCGG AAAA-  
 CGCGGGGG-3'; : 5'-CCCCGCG  
 AACCGCCAAGGGGA AC-3')  
 (10 HE E , H 7.5, 100 C ,  
 5 C<sub>2</sub>) 20 μ  
 95 4 C  
 0.1 C / .  
 147- 601 ( 601) D A  
*E. coli*  
 (65, 66). B  
 147- 601 D A  
 EGF - 1 (A )  
 147- D A  
 E ,  
 ( EG )  
 147- 601 D A 5'-C GGAGAA CCC-  
 GG GCCGAGGCCGC CAA GG CG AGACA-  
 GC C AGCACCGC AAACGCACG ACGCG-  
 C G CCCCCGCG AACCGCCAAGGGG-  
 A AC CCC AG C CCAGGCACG G CAC-  
 A A A ACA CC G -3'.

**Cryo-EM sample preparation**  
 CAF-1 150  
 HD (CAF1- C)  
 H3-H4 1:2.5  
 A-500,  
 30 H  
 16/60 200  
 10 / CAF1-  
 C-H3-H4 D A<sub>30</sub>

1:1.5 A-500,  
 B(20 HE E , H7.5,  
 50 C, 1 D ) 4 C 36 .  
 CAF1-FC-H3-H4-D A30  
 CAF1- C  
 6 10/300 G  
 (GE H )  
 CAF-1, H3-  
 H4, 601 D A (D A<sub>147</sub>)  
 CAF-1,  
 H3-H4, D A<sub>147</sub>- 1:2.5:1  
 A-2000. B  
 4 C 36  
 1 / 200 μ ,  
 G- F (67).  
 12- 10 30%  
 B 0 0.15%  
 E - ( -A ). A  
 4 C 16 38,000  
 40 (B C ) ,  
 25.  
 500 μ  
 8%  
 E  
 A-50,  
 A-500 C  
 50 -E  
 300  
 2/1 C /A  
 ( C , )  
 CAF1- C-H3-H4-D A<sub>30</sub>, CAF1-FC-H3-H4-D A<sub>30</sub>,  
 CAF1- C-H3-H4-D A<sub>147</sub>-  
 300 2/1  
 CAF1- C-H3-H4-D A<sub>147</sub>-  
 G 950 A  
 2/A 60 .A.3-μ  
 0.4 /  
 A  
 10 ,  
 ( 55 , ,GE H  
 ) 3 4.5 ,  
 FE  
 ( F ).A -E  
 10 C. 100%  
**Cryo-EM data acquisition, image processing,  
 and 3D reconstruction**  
 C -E FE  
 A  
 G F  
 200 130,000.  
 G B  
 2  
 20  
 1-  
 (0.5-  
 ). -1.0  
 -1.5 μ . E 5 ,  
 50 /<sup>2</sup>

( , 8.9 / / ) 32  
 A  
 CAF1- C-H3-H4  
 D A<sub>30</sub> . 3. A  
 23,996  
 A C (68).  
 (C F)  
 A C. G (69).  
 19,607  
 A C  
 2D  
 A C,  
 2D  
 19,430,612  
 2,269,295  
 ( )  
 CAF1- C-H3-  
 H4 .A  
 ( ) ,  
 .F  
 , 927,863  
 -3.0 (70)  
 (71)  
 2 . 3D  
 400,801  
 3D  
 304,368  
 A C  
 , 3.9-  
 3.8 .F  
 , 53,708  
 -3.0 3D  
 , 24,904  
 7.2 CAF1- C-H3-H4  
 .F C2  
 6.1  
 F CAF1-FC-H3-H4-D A<sub>30</sub> ,  
 . 4. 15,893  
 A C  
 C F  
 A C.  
 14,532  
 A C  
 2D  
 .A 4,999,183

Downloaded from https://www.science.org at Institute of Biophysics, CAS on September 15, 2025



- - - - - D A - - - - -  
- φ 174 F D A ( EB,  
3021 ) 100 - , D A  
- ( - - - , 2240A ) - - -  
- 10 - -HC, H 7.5, 125  
- C, 2 - - C

... , A- EB  
 D A (E7645)  
 ... A  
 D A (CE- )  
 : 15 -HC, H 7.5, 0.5  
 EG- ( B ), 0.1 C  
 ( -A ), 0.5 H A ( -A ),  
 10 ( -A )  
 45 D A  
 (1.1) 10 -HC,  
 H 7.5, D A  
 C1 ( ).  
 μ  
 1 B & (5  
 -HC H 7.5, 0.5 ED A, 1 C,  
 0.05% -20) 2  
 B &  
 1:1 D A  
 45 , &  
 1 E 0.05% -20,  
 10 -HC, H 7.5  
 10 μ H<sub>2</sub>  
 98 C 10 , 16 C  
 D A C  
 1 A  
 ( 38) B 2 (79)  
 Homo sapiens  
 DA (80) 120  
 180 10-  
 CE-  
 CE-  
 D A  
 CE-  
 D A  
 E A  
 C CF-  
 1000-  
 C CF  
 (C )  
 G E (GE)  
 (G 4640493) (81)

Molecular weight determination by SEC-MALS

A DA HE E 18-  
 ( )  
 A H C  
 6 10/300 G  
 (GE H ).  
 20  
 -HC, H 7.5, 125 C, 2%  
 12  
 B A  
 1 / F  
 CAF-1 CAF-1-H3-H4  
 D A<sub>30</sub>  
 1 /  
 0.5 /  
 D A A  
 A A  
**Single-molecule FOMT analysis**  
 A  
 159- D A  
 C D A  
 (543) Sty  
 147- 601 D A Bsa  
 (2 μ , D )  
 150 C 8  
 ( -A , 2) 5  
 100 μ  
 (0.1 / , ) B  
 4 4 C  
 100 μ  
 10 / B A, 1 ED A,  
 H 8.0, 10 /  
 F127 ( -A , 2443),  
 3 3- 4 C  
 F (54, 82),  
 F .6D,  
 (83). F  
 8- D A  
 (D , 65601)  
 (82, 84),  
 0.45  
 1.8  
 A 1  
 F (50 C, 25 HE E ,  
 H 7.5, 0.1 ED A, 0.025% EG, 0.025%  
 H, 1 / B A), 100 μ  
 D A (3 /μ ) F  
 20  
 200 μ F  
 ( 1) F  
 20 , 200 μ  
 F

1-H3H4 (200 )  
 CAF1-FC-H3-H4 (50 )  
 (50 C, 25  
 HE E , H 7.5, 0.1 ED A, 0.025% EG, 0.025%  
 H, 1 / B A) 4 C 30  
 100  
 A G -E CCD  
 500 H 4  
 ( A 60 ,  
 A 1.42, )  
 (x, y, z) 0.7  
 (x, y) R  
 :  

$$x_i \cdot y_i \cdot R = (x_i - x)^2 + (y_i - y)^2 - R^2 \quad (1)$$

$$\vec{b}, \vec{x}: \begin{matrix} x_1 & y_1 & 1 \\ x_2 & y_2 & 1 \\ \dots & \dots & \dots \\ x_n & y_n & 1 \end{matrix} \quad A = \begin{matrix} x_1^2 + y_1^2 \\ x_2^2 + y_2^2 \\ \dots \\ x_n^2 + y_n^2 \end{matrix} \quad \vec{b} = \begin{matrix} 2x_c \\ 2y_c \\ r^2 - x_c^2 - y_c^2 \end{matrix} \quad \vec{x} = \begin{matrix} x_1 & y_1 \\ x_2 & y_2 \\ \dots & \dots \\ x_n & y_n \end{matrix} \quad A \vec{x} = \vec{b} \quad (3)$$

$$\vec{x} = A^{-1} A \vec{b} \quad (4)$$

$$\Delta \theta_{i,i+1} = \frac{\vec{r}_i \cdot \vec{r}_{i+1}}{r_i r_{i+1}} \quad (5)$$

$$\theta_k = \begin{matrix} k-1 \\ i=1 \end{matrix} \Delta \theta_{i,i+1}, \quad \begin{matrix} \Delta \theta_{i,i+1} \\ k=1 \end{matrix} \quad (6)$$

(r<sub>i</sub>, φ<sub>i</sub>)

Downloaded from https://www.science.org at Institute of Biophysics, CAS on September 15, 2025

$$r_i = (x_i - x_c)^2 + (y_i - y_c)^2 \quad (7)$$

$$\phi_i = \frac{y_i - y_c}{x_i - x_c} \quad (8)$$

$$F_{\text{MSA}} \quad (85)$$

### EMSA

E A ( 20 μ ),  
 0.5 μ 147- D A 0.5, 1,  
 2.5, 5, 10 μ 60ΔC 48,  
 20 -HC, H 7.5, 50  
 C, 1 D, 30, 6%  
 0.5 BE 120 50  
 B G ( F )  
 G D E  
 (B - ).

### Quantification and statistical analysis

(68).

(64).

(A A)

p D A

### REFERENCES AND NOTES

- K. Luger, A. W. M. der, R. K. Richmond, D. F. Sargent, T. J. Richmond, Crystal structure of the nucleosome core particle at 2.8 Å resolution. *Nature* **389**, 251–260 (1997). doi: [10.1038/38444](https://doi.org/10.1038/38444); pmid: [9305837](https://pubmed.ncbi.nlm.nih.gov/9305837/)
- A. Serra-Cardona, Z. Zhang, Replication-coupled nucleosome assembly in the passage of epigenetic information and cell identity. *Trends Biochem. Sci.* **43**, 136–148 (2018). doi: [10.1016/j.tibs.2017.12.003](https://doi.org/10.1016/j.tibs.2017.12.003); pmid: [29292063](https://pubmed.ncbi.nlm.nih.gov/29292063/)
- A. Groth, W. Rocha, A. Verreault, G. Almouzni, Chromatin challenges during DNA replication and repair. *Cell* **128**, 721–733 (2007). doi: [10.1016/j.cell.2007.01.030](https://doi.org/10.1016/j.cell.2007.01.030); pmid: [17320509](https://pubmed.ncbi.nlm.nih.gov/17320509/)
- M. Xu et al., Partitioning of histone H3-H4 tetramers during DNA replication-dependent chromatin assembly. *Science* **328**, 94–98 (2010). doi: [10.1126/science.1178994](https://doi.org/10.1126/science.1178994); pmid: [20360108](https://pubmed.ncbi.nlm.nih.gov/20360108/)
- C. Yu et al., A mechanism for preventing asymmetric histone segregation onto replicating DNA strands. *Science* **361**, 1386–1389 (2018). doi: [10.1126/science.aat8849](https://doi.org/10.1126/science.aat8849); pmid: [30115745](https://pubmed.ncbi.nlm.nih.gov/30115745/)
- N. Petryk et al., MCM2 promotes symmetric inheritance of modified histones during DNA replication. *Science* **361**, 1389–1392 (2018). doi: [10.1126/science.aau0294](https://doi.org/10.1126/science.aau0294); pmid: [30115746](https://pubmed.ncbi.nlm.nih.gov/30115746/)
- S. Smith, B. Stillman, Purification and characterization of CAF-1, a human cell factor required for chromatin assembly during DNA replication in vitro. *Cell* **58**, 15–25 (1989). doi: [10.1016/0092-8674\(89\)90398-X](https://doi.org/10.1016/0092-8674(89)90398-X); pmid: [2546672](https://pubmed.ncbi.nlm.nih.gov/2546672/)
- S. Smith, B. Stillman, Stepwise assembly of chromatin during DNA replication in vitro. *EMBO J.* **10**, 971–980 (1991). doi: [10.1002/j.1460-2075.1991.tb08031.x](https://doi.org/10.1002/j.1460-2075.1991.tb08031.x); pmid: [1849080](https://pubmed.ncbi.nlm.nih.gov/1849080/)
- P. D. Kaufman, R. Kobayashi, N. Kessler, B. Stillman, The p150 and p60 subunits of chromatin assembly factor I: A molecular link between newly synthesized histones and DNA replication. *Cell* **81**, 1105–1114 (1995). doi: [10.1016/S0092-8674\(05\)80015-7](https://doi.org/10.1016/S0092-8674(05)80015-7); pmid: [7600578](https://pubmed.ncbi.nlm.nih.gov/7600578/)
- Z. Zhang, K. Shibahara, B. Stillman, PCNA connects DNA replication to epigenetic inheritance in yeast. *Nature* **408**, 221–225 (2000). doi: [10.1038/35041601](https://doi.org/10.1038/35041601); pmid: [11089978](https://pubmed.ncbi.nlm.nih.gov/11089978/)
- K. Shibahara, B. Stillman, Replication-dependent marking of DNA by PCNA facilitates CAF-1-coupled inheritance of chromatin. *Cell* **96**, 575–585 (1999). doi: [10.1016/S0092-8674\(00\)80661-3](https://doi.org/10.1016/S0092-8674(00)80661-3); pmid: [10052459](https://pubmed.ncbi.nlm.nih.gov/10052459/)
- J. K. Tyler et al., The RCAF complex mediates chromatin assembly during DNA replication and repair. *Nature* **402**, 555–560 (1999). doi: [10.1038/990147](https://doi.org/10.1038/990147); pmid: [10591219](https://pubmed.ncbi.nlm.nih.gov/10591219/)
- J. A. Sharp, E. T. Fouts, D. C. Krawitz, P. D. Kaufman, Yeast histone deposition protein Asf1p requires Hir proteins and PCNA for heterochromatic silencing. *Curr. Biol.* **11**, 463–473 (2001). doi: [10.1016/S0960-9822\(01\)00140-3](https://doi.org/10.1016/S0960-9822(01)00140-3); pmid: [11412995](https://pubmed.ncbi.nlm.nih.gov/11412995/)
- M. Hoek, B. Stillman, Chromatin assembly factor 1 is essential and couples chromatin assembly to DNA replication in vivo. *Proc. Natl. Acad. Sci. U.S.A.* **100**, 12183–12188 (2003). doi: [10.1073/pnas.1635158100](https://doi.org/10.1073/pnas.1635158100); pmid: [14519857](https://pubmed.ncbi.nlm.nih.gov/14519857/)
- S. Enomoto, P. D. McCune-Zierath, M. Gerami-Nejad, M. A. Sanders, J. Berman, RLF2, a subunit of yeast chromatin assembly factor-1, is required for telomeric chromatin function in vivo. *Genes Dev.* **11**, 358–370 (1997). doi: [10.1101/gad.11.3.358](https://doi.org/10.1101/gad.11.3.358); pmid: [9030688](https://pubmed.ncbi.nlm.nih.gov/9030688/)
- P. D. Kaufman, R. Kobayashi, B. Stillman, Ultraviolet radiation sensitivity and reduction of telomeric silencing in *Saccharomyces cerevisiae* cells lacking chromatin assembly factor-1. *Genes Dev.* **11**, 345–357 (1997). doi: [10.1101/gad.11.3.345](https://doi.org/10.1101/gad.11.3.345); pmid: [9030687](https://pubmed.ncbi.nlm.nih.gov/9030687/)
- Q. Li et al., Acetylation of histone H3 lysine 56 regulates replication-coupled nucleosome assembly. *Cell* **134**, 244–255 (2008). doi: [10.1016/j.cell.2008.06.018](https://doi.org/10.1016/j.cell.2008.06.018); pmid: [18662540](https://pubmed.ncbi.nlm.nih.gov/18662540/)
- H. Tagami, D. Ray-Gallet, G. Almouzni, Y. Nakatani, Histone H3.1 and H3.3 complexes mediate nucleosome assembly pathways dependent or independent of DNA synthesis. *Cell* **116**, 51–61 (2004). doi: [10.1016/S0092-8674\(03\)01064-X](https://doi.org/10.1016/S0092-8674(03)01064-X); pmid: [14718166](https://pubmed.ncbi.nlm.nih.gov/14718166/)
- K. Ahmad, S. Henikoff, The histone variant H3.3 marks active chromatin by replication-independent nucleosome assembly. *Mol. Cell* **9**, 1191–1200 (2002). doi: [10.1016/S1097-2765\(02\)00542-7](https://doi.org/10.1016/S1097-2765(02)00542-7); pmid: [12086617](https://pubmed.ncbi.nlm.nih.gov/12086617/)
- E. Martini, D. M. Roche, K. Marheineke, A. Verreault, G. Almouzni, Recruitment of phosphorylated chromatin assembly factor 1 to chromatin after UV irradiation of human cells. *J. Cell Biol.* **143**, 563–575 (1998). doi: [10.1083/jcb.143.3.563](https://doi.org/10.1083/jcb.143.3.563); pmid: [9813080](https://pubmed.ncbi.nlm.nih.gov/9813080/)
- P. Ridgway, G. Almouzni, CAF-1 and the inheritance of chromatin states: At the crossroads of DNA replication and repair. *J. Cell Sci.* **113**, 2647–2658 (2000). doi: [10.1242/jcs.113.15.2647](https://doi.org/10.1242/jcs.113.15.2647); pmid: [10893180](https://pubmed.ncbi.nlm.nih.gov/10893180/)
- S. Cheloufi, K. Hochedlinger, Emerging roles of the histone chaperone CAF-1 in cellular plasticity. *Curr. Opin. Genet. Dev.* **46**, 83–94 (2017). doi: [10.1016/j.cde.2017.06.004](https://doi.org/10.1016/j.cde.2017.06.004); pmid: [28692904](https://pubmed.ncbi.nlm.nih.gov/28692904/)
- A. Verreault, P. D. Kaufman, R. Kobayashi, B. Stillman, Nucleosome assembly by a complex of CAF-1 and acetylated histones H3/H4. *Cell* **87**, 95–104 (1996). doi: [10.1016/S0092-8674\(00\)81326-4](https://doi.org/10.1016/S0092-8674(00)81326-4); pmid: [8858152](https://pubmed.ncbi.nlm.nih.gov/8858152/)
- P. V. Sauer et al., Mechanistic insights into histone deposition and nucleosome assembly by the chromatin assembly factor-1. *Nucleic Acids Res.* **46**, 9907–9917 (2018). doi: [10.1093/nar/gky823](https://doi.org/10.1093/nar/gky823); pmid: [30239791](https://pubmed.ncbi.nlm.nih.gov/30239791/)
- T. Rolef Ben-Shahar et al., Two fundamentally distinct PCNA interaction peptides contribute to chromatin assembly factor 1 function. *Mol. Cell Biol.* **29**, 6353–6365 (2009). doi: [10.1128/MCB.01051-09](https://doi.org/10.1128/MCB.01051-09); pmid: [19822659](https://pubmed.ncbi.nlm.nih.gov/19822659/)
- A. Volk, J. D. Crispino, The role of the chromatin26oon 606p2fac3(subunit6p2f21.906HAF1b6.6p2760.6(in)-fac3(hsomostasis))JTJO-1.2838TD((and))

- tetrasome assembly in the wake of DNA replication. *eLife* **6**, e22799 (2017). doi: [10.7554/eLife.22799](https://doi.org/10.7554/eLife.22799); pmid: [28315523](https://pubmed.ncbi.nlm.nih.gov/28315523/)
53. K. Nozawa *et al.*, Cryo-electron microscopy structure of the H3-H4 octasome: A nucleosome-like particle without histones H2A and H2B. *Proc. Natl. Acad. Sci. U.S.A.* **119**, e2206542119 (2022). doi: [10.1073/pnas.2206542119](https://doi.org/10.1073/pnas.2206542119); pmid: [36322721](https://pubmed.ncbi.nlm.nih.gov/36322721/)
  54. R. Vlijm *et al.*, Nucleosome assembly dynamics involve spontaneous fluctuations in the handedness of tetrasomes. *Cell Rep.* **10**, 216–225 (2015). doi: [10.1016/j.celrep.2014.12.022](https://doi.org/10.1016/j.celrep.2014.12.022); pmid: [25578730](https://pubmed.ncbi.nlm.nih.gov/25578730/)
  55. C. Rouillon *et al.*, CAF-1 deposits newly synthesized histones during DNA replication using distinct mechanisms on the leading and lagging strands. *Nucleic Acids Res.* **51**, 3770–3792 (2023). doi: [10.1093/nar/gkad171](https://doi.org/10.1093/nar/gkad171); pmid: [36942484](https://pubmed.ncbi.nlm.nih.gov/36942484/)
  56. J. Fei *et al.*, The prenucleosome, a stable conformational isomer of the nucleosome. *Genes Dev.* **29**, 2563–2575 (2015). doi: [10.1101/gad.272633.115](https://doi.org/10.1101/gad.272633.115); pmid: [26680301](https://pubmed.ncbi.nlm.nih.gov/26680301/)
  57. A. Hamiche *et al.*, Interaction of the histone (H3-H4)<sub>2</sub> tetramer of the nucleosome with positively supercoiled DNA minicircles: Potential flipping of the protein from a left- to a right-handed superhelical form. *Proc. Natl. Acad. Sci. U.S.A.* **93**, 7588–7593 (1996). doi: [10.1073/pnas.93.15.7588](https://doi.org/10.1073/pnas.93.15.7588); pmid: [8755519](https://pubmed.ncbi.nlm.nih.gov/8755519/)
  58. T. Furuyama, S. Henikoff, Centromeric nucleosomes induce positive DNA supercoils. *Cell* **138**, 104–113 (2009). doi: [10.1016/j.cell.2009.04.049](https://doi.org/10.1016/j.cell.2009.04.049); pmid: [19596238](https://pubmed.ncbi.nlm.nih.gov/19596238/)
  59. X. Ming *et al.*, Kinetics and mechanisms of mitotic inheritance of DNA methylation and their roles in aging-associated methylome deterioration. *Cell Res.* **30**, 980–996 (2020). doi: [10.1038/s41422-020-0359-9](https://doi.org/10.1038/s41422-020-0359-9); pmid: [32581343](https://pubmed.ncbi.nlm.nih.gov/32581343/)
  60. Z. Otwinowski, W. Minor, Processing of X-ray diffraction data collected in oscillation mode. *Methods Enzymol.* **276**, 307–326 (1997). doi: [10.1016/S0076-6879\(97\)76066-X](https://doi.org/10.1016/S0076-6879(97)76066-X); pmid: [27754618](https://pubmed.ncbi.nlm.nih.gov/27754618/)
  61. A. J. McCoy *et al.*, Phaser crystallographic software. *J. Appl. Crystallogr.* **40**, 658–674 (2007). doi: [10.1107/S0021889807021206](https://doi.org/10.1107/S0021889807021206); pmid: [19461840](https://pubmed.ncbi.nlm.nih.gov/19461840/)
  62. P. Emsley, K. Cowtan, Coot: Model-building tools for molecular graphics. *Acta Crystallogr. D Biol. Crystallogr.* **60**, 2126–2132 (2004). doi: [10.1107/S0907444904019158](https://doi.org/10.1107/S0907444904019158); pmid: [15572765](https://pubmed.ncbi.nlm.nih.gov/15572765/)
  63. P. D. Adams *et al.*, PHENIX: A comprehensive Python-based system for macromolecular structure solution. *Acta Crystallogr. D Biol. Crystallogr.* **66**, 213–221 (2010). doi: [10.1107/S0907444909052925](https://doi.org/10.1107/S0907444909052925); pmid: [20124702](https://pubmed.ncbi.nlm.nih.gov/20124702/)
  64. V. B. Chen *et al.*, MolProbity: All-atom structure validation for macromolecular crystallography. *Acta Crystallogr. D Biol. Crystallogr.* **66**, 12–21 (2010). doi: [10.1107/S0907444909042073](https://doi.org/10.1107/S0907444909042073); pmid: [20057044](https://pubmed.ncbi.nlm.nih.gov/20057044/)
  65. P. N. Dyer *et al.*, Reconstitution of nucleosome core particles from recombinant histones and DNA. *Methods Enzymol.* **375**, 23–44 (2004). doi: [10.1016/S0076-6879\(03\)75002-2](https://doi.org/10.1016/S0076-6879(03)75002-2); pmid: [14870657](https://pubmed.ncbi.nlm.nih.gov/14870657/)
  66. P. T. Lowary, J. Widom, New DNA sequence rules for high affinity binding to histone octamer and sequence-directed nucleosome positioning. *J. Mol. Biol.* **276**, 19–42 (1998). doi: [10.1006/jmbi.1997.1494](https://doi.org/10.1006/jmbi.1997.1494); pmid: [9514715](https://pubmed.ncbi.nlm.nih.gov/9514715/)
  67. B. Kastner *et al.*, GraFix: Sample preparation for single-particle electron cryomicroscopy. *Nat. Methods* **5**, 53–55 (2008). doi: [10.1038/nmeth1139](https://doi.org/10.1038/nmeth1139); pmid: [18157137](https://pubmed.ncbi.nlm.nih.gov/18157137/)
  68. A. Punjani, J. L. Rubinstein, D. J. Fleet, M. A. Brubaker, cryoSPARC: Algorithms for rapid unsupervised cryo-EM structure determination. *Nat. Methods* **14**, 290–296 (2017). doi: [10.1038/nmeth.4169](https://doi.org/10.1038/nmeth.4169); pmid: [28165473](https://pubmed.ncbi.nlm.nih.gov/28165473/)
  69. K. Zhang, Gctf: Real-time CTF determination and correction. *J. Struct. Biol.* **193**, 1–12 (2016). doi: [10.1016/j.jsb.2015.11.003](https://doi.org/10.1016/j.jsb.2015.11.003); pmid: [26592709](https://pubmed.ncbi.nlm.nih.gov/26592709/)
  70. J. Zivanov *et al.*, New tools for automated high-resolution cryo-EM structure determination in RELION-3. *eLife* **7**, e42166 (2018). doi: [10.7554/eLife.42166](https://doi.org/10.7554/eLife.42166); pmid: [30412051](https://pubmed.ncbi.nlm.nih.gov/30412051/)
  71. D. Asarnow, E. Palovcak, Y. Cheng, UCSF pyem v0.5. *Zenodo* (2019). doi: [10.5281/zenodo.3576630](https://doi.org/10.5281/zenodo.3576630)
  72. E. F. Pettersen *et al.*, UCSF Chimera—A visualization system for exploratory research and analysis. *J. Comput. Chem.* **25**, 1605–1612 (2004). doi: [10.1002/jcc.20084](https://doi.org/10.1002/jcc.20084); pmid: [15264254](https://pubmed.ncbi.nlm.nih.gov/15264254/)
  73. T. D. Goddard *et al.*, UCSF ChimeraX: Meeting modern challenges in visualization and analysis. *Protein Sci.* **27**, 14–25 (2018). doi: [10.1002/pro.3235](https://doi.org/10.1002/pro.3235); pmid: [28710774](https://pubmed.ncbi.nlm.nih.gov/28710774/)
  74. A. Osakabe *et al.*, Nucleosome formation activity of human somatic nuclear autoantigenic sperm protein (sNASP). *J. Biol. Chem.* **285**, 11913–11921 (2010). doi: [10.1074/jbc.M109.083238](https://doi.org/10.1074/jbc.M109.083238); pmid: [20167597](https://pubmed.ncbi.nlm.nih.gov/20167597/)
  75. J. Xiong *et al.*, Cooperative action between SALL4A and TET proteins in stepwise oxidation of 5-methylcytosine. *Mol. Cell* **64**, 913–925 (2016). doi: [10.1016/j.molcel.2016.10.013](https://doi.org/10.1016/j.molcel.2016.10.013); pmid: [27840027](https://pubmed.ncbi.nlm.nih.gov/27840027/)
  76. S. Ramachandran, S. Henikoff, Transcriptional regulators compete with nucleosomes post-replication. *Cell* **165**, 580–592 (2016). doi: [10.1016/j.cell.2016.02.062](https://doi.org/10.1016/j.cell.2016.02.062); pmid: [27062929](https://pubmed.ncbi.nlm.nih.gov/27062929/)
  77. S. Liu *et al.*, RPA binds histone H3-H4 and functions in DNA replication-coupled nucleosome assembly. *Science* **355**, 415–420 (2017). doi: [10.1126/science.aah4712](https://doi.org/10.1126/science.aah4712); pmid: [28126821](https://pubmed.ncbi.nlm.nih.gov/28126821/)
  78. J. Yu *et al.*, Analysis of local chromatin states reveals gene transcription potential during mouse neural progenitor cell differentiation. *Cell Rep.* **32**, 107953 (2020). doi: [10.1016/j.celrep.2020.107953](https://doi.org/10.1016/j.celrep.2020.107953); pmid: [32726618](https://pubmed.ncbi.nlm.nih.gov/32726618/)
  79. B. Langmead, S. L. Salzberg, Fast gapped-read alignment with Bowtie 2. *Nat. Methods* **9**, 357–359 (2012). doi: [10.1038/nmeth.1923](https://doi.org/10.1038/nmeth.1923); pmid: [22388286](https://pubmed.ncbi.nlm.nih.gov/22388286/)
  80. K. Chen *et al.*, DANPOS: Dynamic analysis of nucleosome position and occupancy by sequencing. *Genome Res.* **23**, 341–351 (2013). doi: [10.1101/gr.142067.112](https://doi.org/10.1101/gr.142067.112); pmid: [23193179](https://pubmed.ncbi.nlm.nih.gov/23193179/)
  81. J. H. I. Haarhuis *et al.*, A Mediator-cohesin axis controls heterochromatin domain formation. *Nat. Commun.* **13**, 754 (2022). doi: [10.1038/s41467-022-28377-7](https://doi.org/10.1038/s41467-022-28377-7); pmid: [35136067](https://pubmed.ncbi.nlm.nih.gov/35136067/)
  82. J. Lipfert, M. Wiggan, J. W. Kerssemakers, F. Pedaci, N. H. Dekker, Freely orbiting magnetic tweezers to directly monitor changes in the twist of nucleic acids. *Nat. Commun.* **2**, 439 (2011). doi: [10.1038/ncomms1450](https://doi.org/10.1038/ncomms1450); pmid: [21863006](https://pubmed.ncbi.nlm.nih.gov/21863006/)
  83. P. Chen *et al.*, Functions of FACT in breaking the nucleosome and maintaining its integrity at the single-nucleosome level. *Mol. Cell* **71**, 284–293.e4 (2018). doi: [10.1016/j.molcel.2018.06.020](https://doi.org/10.1016/j.molcel.2018.06.020); pmid: [30029006](https://pubmed.ncbi.nlm.nih.gov/30029006/)
  84. A. J. te Velthuis, J. W. Kerssemakers, J. Lipfert, N. H. Dekker, Quantitative guidelines for force calibration through spectral analysis of magnetic tweezers data. *Biophys. J.* **99**, 1292–1302 (2010). doi: [10.1016/j.bpj.2010.06.008](https://doi.org/10.1016/j.bpj.2010.06.008); pmid: [20713015](https://pubmed.ncbi.nlm.nih.gov/20713015/)
  85. Z. Li, Code for analysis and plotting data from freely orbiting magnetic tweezers (1.0). *Zenodo* (2023); <https://doi.org/10.5281/zenodo.8166291>.

#### ACKNOWLEDGMENTS

We thank B. Zhu, X. Huang, and staff members at the Center for Biological Imaging (CBI) of the Institute of Biophysics (IBP), Chinese Academy of Sciences, for support in cryo-EM data collection; X. Yu at IBP for technical support with SEC-MALS analysis; and staff scientists at Shanghai Synchrotron Radiation Facility (SSRF) beamlines BL17U and BL19U for assistance in x-ray data collection. We also thank M. Jin and Y. Cong at Shanghai

Institute of Biochemistry and Cell Biology and M. Zhou, Y. Wang, P. Zhu, and D. Cao at IBP for participation during the early stages of this study. **Funding:** This work was funded by Ministry of Science and Technology of China grant 2019YFA0508900 (R.-M.X.); National Natural Science Foundation of China grants 31991162, 91853204, and 92153302 (R.-M.X.) and 32288102 (B.Z.); Ministry of Science and Technology of China grants 2018YFE0203300 and 2017YFA0506600 (C.-P.L.); Chinese Academy of Sciences Strategic Priority Research Program XDB37010100 (R.-M.X.) and XDB39010100 (B.Z.); Chinese Academy of Sciences Youth Innovation Promotion Association grants 2018125 (C.-P.L.), 2017131 (Z.Y.), 2020097 (J.X.), and 2017133 (Z.Q.Z.); and the New Cornerstone Investigator Program (B.Z.). **Author contributions:** Conceptualization: R.-M.X., C.-P.L., Z.G.Z.; Methodology: C.-P.L., C.Y., M.W., W.L., Z.Q.Z., X.Z., B.Z., G.L., R.-M.X.; Investigation: C.-P.L., Z.Y., J.X., J.H., A.S., D.D., J.Y., P.H., K.Z., Z.L.; Visualization: C.-P.L., C.Y., M.W.; Funding acquisition: R.-M.X., C.-P.L.; Project administration: R.-M.X., N.Y.; Supervision: R.-M.X., G.L., B.Z., N.Y., W.L.; Writing – original draft: C.-P.L., R.-M.X.; Writing – review and editing: All authors. **Competing interests:** The authors declare that they have no competing interests. **Data and materials availability:** All data and materials used in this study are available for academic purposes upon request. Atomic coordinates and associated structure factors from crystallographic studies have been deposited in the Protein Data Bank (PDB) under accession numbers 7Y5K, 7Y5L, and 7Y5O for the models belonging to the C222<sub>1</sub>, C2, and P2<sub>1</sub> space groups, respectively. EM maps and fitted structural models have been deposited in the Electron Microscopy Data Bank (EMDB) and PDB with the following accession information: the 1:1 CAF1LC-H3-H4 complex, EMD-33625 and 7Y5U; the 2:2 CAF1LC-H3-H4 complex, EMD-33626 and 7Y5V; the monomeric CAF-1-H3-H4 complex, EMD-35661 and 8IQG; the dimeric CAF-1-H3-H4 complex, EMD-35660 (composite map), EMD-35708 (consensus map), EMD-35709 (local map for protomer I), EMD-35710 (local map for protomer II), and 8IQF; left-handed di-tetrasome, EMD-33627 and 7Y5W; CAF1LC bound right-handed di-tetrasome, EMD-33630 and 7Y60; right-handed di-tetrasome bound by two CAF1LC complexes, EMD-33631 and 7Y61; the single CAF-1-bound right-handed di-tetrasome, EMD-36013 and 8J6S; and the double CAF-1-bound right-handed di-tetrasome,